Published in final edited form as:
Biochemistry. 2007 December 4; 46(48): 13874–13881. doi:10.1021/bi700851z.

Steric and Electrostatic Effects in DNA Synthesis by the SOS-Induced DNA Polymerases II and IV of *Escherichia coli*

Adam P. Silverman[1], **Qingfei Jiang**[2], **Myron F. Goodman**[2,*], and **Eric T. Kool**[1,*]

1 *Department of Chemistry, Stanford University, Stanford, CA 94305-5080*

2 *Department of Biological Sciences, University of Southern California, Los Angeles, CA 90089-2910*

Abstract

The SOS-induced DNA polymerases II and IV of *Escherichia coli* play important roles in processing lesions that occur in genomic DNA. Here we study how electrostatic and steric effects play different parts in influencing the efficiency and fidelity of DNA synthesis by these two enzymes. These effects were probed by the use of nonpolar shape analogs of thymidine, in which substituted toluenes replace the polar thymine base. Comparison of thymine with nonpolar analogs was made to evaluate the importance of hydrogen bonding in the polymerase active sites, while comparisons among a set of variably-sized thymine analogs was used to measure the role of steric effects in the two enzymes. Steady-state kinetics measurements were carried out to evaluate activities for nucleotide insertion and extension. The results showed that both enzymes inserted nucleotides opposite nonpolar template bases with moderate to low efficiency, suggesting that both polymerases benefit from hydrogen bonding or other electrostatic effects involving the template base. Surprisingly, however, pol II inserted nonpolar nucleotide (dNTP) analogs into a primer strand with high (wild-type) efficiency, while pol IV handled them with extremely low efficiency. Base pair extension studies showed that both enzymes bypass non-hydrogen bonding template bases with moderately low efficiency, suggesting a possible beneficial role of minor groove hydrogen bonding interactions at the N-1 position. Measurement of the two polymerases' sensitivity to steric size changes showed that both enzymes were relatively flexible, yielding only small kinetic differences with increases or decreases in nucleotide size. Comparisons are made to recent data for DNA pol I (Klenow fragment), the archaeal polymerase Dpo4, and human pol kappa.

Keywords

polymerase; isostere; translesion synthesis; DNA damage; nonpolar isostere

Introduction

DNA damage from reactive oxygen species, UV light, or chemical carcinogens can lead to structural changes in the bases, resulting in modified bases such as 8-oxo-guanine, and to adducts such as those of *N*-2-acetylaminofluorene and benzo[*a*]pyrene diol epoxide. Structurally altered bases often block the progression of replicative DNA polymerases such as Pol III of *E. coli* (1). In order for replication to continue, specialized "translesion synthesis" enzymes that can progress past the damage are required. In response to DNA damage, a biological response (the SOS response) is induced in *E. coli*, leading to upregulation of over 40 genes, including DNA polymerases II, IV, and V (2). Pol II is a high-fidelity polymerase

*To whom correspondence should be addressed. mgoodman@usc.edu; Tel 213-740-5190; Fax 213-740-8631; kool@stanford.edu; Tel 650 724 4741; Fax 650 725 0259.

that has a 3′-exonuclease proofreading domain, while pol IV and pol V are more error-prone than pol II, leading to mispairing errors approximately once per 10^3 – 10^4 base pairs (3,4). Specialized roles for these polymerases have been proposed over the past decade. While pol V is responsible for the catalysis of error-prone translesion synthesis, pol II is used for error-free replication restart, and pol IV is responsible for generating nontargeted frameshift mutations while rescuing stalled replication forks (5). The polymerase utilized at a given site may depend on the type of damage; for example, DNA pol IV has been shown to afford translesion synthesis past benzo(*a*)pyrene diol epoxide adducts to guanine, while pol II can replicate past *N*-2-acetylaminofluorene adducts (6).

Adaptive mutations, such as *lacZ* adaptive frameshift mutations and other -1 frameshift mutations, are attributed to pol IV, which has constitutive cellular levels five times higher than pol II (7). Pol II is conversely responsible for decreasing the number of adaptive mutations through error-free replication and its 3′-exonuclease domain (8,9). Thus, pol II and pol IV are believed to carry out a mutational balancing act in order to maximize cellular fitness.

In order to better understand how polymerases to deal with damaged DNA, it is important to consider the enzymes' ability to accept non-canonical nucleoside substrates. A number of factors are involved in recognition of substrates, including base and base pair size and shape (steric effects), as well as hydrogen bonding and solvation of the dNTP or template base (electrostatic effects) (10). Research in the past decade has demonstrated that Watson-Crick hydrogen bonding is in some cases not required for polymerase activity (11–13), particularly for A family high-fidelity enzymes. This has led to the hypothesis that steric effects play a dominant role in determining the fidelity of such enzymes (10,14,15). Studies on the incorporation efficiencies and fidelities of nonpolar nucleoside isosteres (16) as well as variously substituted fluorinated and methylated base mimics have shown that active site size and shape can play critical roles in polymerase activity and fidelity (17–19) and practical applications of shape-selective, non-hydrogen bonded base pairs have begun to be developed recently (20).

To test steric effects with DNA polymerases in a systematic way, we recently described a set of nonpolar thymidine analogs (Figure 1) that are shaped nearly identically to thymidine but use structural mimics (toluene H, difluorotoluene F, dichlorotoluene L, dibromotoluene B, and diiodotoluene I) that differ in size by about 1 Å across the entire series (21,22). Kinetics studies replacing natural template bases or nucleoside triphosphates with the variably-sized thymidine analogs using *E. coli* DNA Pol I Klenow fragment (Kf *exo*-) (23) and T7 DNA polymerase (24) demonstrated large differences in fidelity and efficiency as the base size was changed, demonstrating a high degree of steric rigidity. A similar result was also observed for this series in an *E. coli* cellular replication assay (23). In contrast to this, a low-fidelity Y family enzyme, Dpo4 DNA polymerase (25), was found to be quite flexible in accepting variably sized analogs, and also showed a strong kinetic preference for hydrogen bonded base pairs over nonpolar analogs. We ascribed the differences in fidelity between these distinct enzyme classes to differences in active site tightness of high-fidelity enzymes to low-fidelity ones, with the notion that repair enzymes need to process structurally altered (damaged or mispaired) substrates, and so can benefit from steric flexibility.

Since pol II and pol IV offer contrasting replication fidelities and different biological roles, it is important to understand what role sterics and electrostatics play in the ability of these polymerases to replicate unnatural or damaged DNA. In this work, we test the active site flexibilities of pol II and pol IV (an exonuclease deficient mutant) using the variably sized nonpolar thymidine analogs, and evaluate their dependence on electrostatic effects. Results for single nucleotide incorporation and extension suggest that differences in active site tightness

play a significant part in the differing fidelities of pol II and pol IV, and the data also reveal the importance of hydrogen bonding and solvation effects for these SOS-induced enzymes.

Results

Single nucleotide insertion kinetics

Single nucleotide insertion experiments were performed using a 23-mer/28-mer primer-template duplex. The primer was 5′ end-labeled with ^{32}P, and products were evaluated on denaturing PAGE gels. Steady-state kinetics were measured by use of varied nucleotide concentrations, and the single nucleotide insertion efficiencies (as V_{max}/K_M) were evaluated for the nonpolar thymidine analog series. The steady-state method measures overall catalytic efficiency without assumptions of which microscopic step in the catalytic cycle is rate limiting; note that mispaired bases or nucleotide analogs may cause changes in which step is limiting.

To evaluate steric and electrostatic effects during base pair synthesis by pol IV, we first studied the efficiency of natural dNTP insertion opposite the variably sized nonpolar thymidine analogs. The data are given in Table 1, and are compared graphically in Figure 2. Results showed that dATP was inserted preferentially opposite these analogs, but only 2- to 12-fold more efficiently than dTTP. This was in strong contrast to natural nucleotides: dATP was inserted opposite T 4200-fold more efficiently than dTTP was, similar to the reported fidelity of pol IV (3). Overall, incorporation of dATP opposite the template base mimics was 10^3- to 10^4-fold less efficient than incorporation of dATP opposite natural thymidine, suggesting that the polar electrostatics of thymine in the T-A pair are important for base pair synthesis by this enzyme. A small size influence (about 8-fold) was observed across the series, with the dichlorotoluene template base analog (dL) giving the greatest incorporation efficiency.

We next carried out the converse experiment, attempting to insert the nonpolar thymidine analogs as dNTPs opposite natural template bases; however, no incorporation of any of the nonnatural dNTPs was observed even at very high enzyme concentrations and long reaction times. We estimate a maximum efficiency (V_{max}/K_m) of 2 or less for this insertion (compared with 2.8×10^5 for dATP insertion opposite dT (Table 1)); thus, insertion of dATP opposite dL was more efficient than dLTP opposite dA by at least a factor of 50, demonstrating substantial asymmetry in the pairing efficiency.

The analogous experiments were then carried out with DNA pol II (Fig. 3; Tables 2 and 3). We used an exonuclease-deficient mutant (D155A/E157A) (27) to follow insertion in the absence of proofreading activity. As with pol IV, pol II was also inefficient at inserting natural dNTPs opposite the nonpolar template base analogs (Fig. 3A). Also like pol IV, there was selectivity for dATP, which was preferred over dTTP by about 40-fold for medium-sized analogs dF and dL, but less than 3-fold for dH, dB, and dI. Overall, dATP was incorporated 10^3- to 10^4-fold less efficiently opposite the unnatural bases compared with opposite thymidine. Some size dependence was observed, with dATP being incorporated opposite dL 30-fold more efficiently than opposite the smallest and largest analogs dH and dI. Poor incorporation was observed for dCTP and dGTP in a somewhat size-dependent manner, with maximum efficiency at dL for dCTP and at dF for dGTP. With natural nucleotides there was much higher fidelity, with a 6100-fold enzymatic preference for insertion of dATP rather than dTTP opposite a template T.

Next we looked at the ability of DNA pol II to insert variably-sized nonpolar dNTPs opposite natural template bases (Figure 3B, Table 3). The results were strikingly different than with pol IV (above): the four largest thymidine triphosphate analogs were inserted opposite adenine by pol II with equal or greater efficiency than natural dTTP was. Indeed, the most efficient nucleotide (dLTP) was inserted 3.6-fold more efficiently than dTTP. The efficiency of

incorporation opposite A was greatest with dLTP and decreased as the base got larger or smaller, decreasing by 154-fold for the smallest nucleotide triphosphate, dHTP. The unnatural dNTPs were incorporated selectively opposite A, except for dHTP which was inserted opposite T about 8-fold better. Selectivity for a template A over a T for the most selective case (dLTP) was slightly less than that of the natural nucleotide dTTP (24-fold vs. 33-fold). Interestingly, incorporation of the analogs opposite the other mismatched bases, C and G, was also highly dependent on base size. Incorporation opposite C increased 240-fold as base size was increased from dHTP to dBTP, and then decreased 15-fold for dITP. A similar, but less dramatic trend was observed for incorporation opposite G, which also peaked with dBTP and varied by about 100-fold across the series.

Extension beyond variably-sized template bases

Because an important function of SOS-induced polymerases is extension beyond damaged or mispaired bases, we proceeded to evaluate steric effects in the extension step, separate from insertion. We measured steady-state kinetics for extension past an A·X base pair, where X is a variably-sized thymidine template base analog, with comparison of results for extension past natural A·T base pairs.

Results for pol IV showed a moderate size dependence in extension past A·X base pairs (Figure 4B, Table 5). The A·L base pair was extended most efficiently, 240-fold less efficiently than an A·T base pair, and the extension efficiency dropped as base pair size was increased or decreased. The poorest extension occurred with the smallest (A·H) and largest (A·I) base pairs, which were extended about four orders of magnitude less efficiently than an A·T pair. Across the entire series, extension efficiencies varied by 48-fold.

Pol II extension results showed that the enzyme, like pol IV, was also poor at extending past unnatural base pairs (Figure 4A, Table 4). Analog A·X base pairs were extended with 2–3 orders of magnitude lower efficiency than natural A·T base pairs. Unlike pol IV extension, however, there was very little effect of base pair size on extension efficiency, as the extension efficiencies across the entire series varied by less than 5-fold.

Discussion

Taken together, our experiments show that both of the SOS-induced polymerases II and IV are only moderately to weakly sensitive to changes in base size, and thus should be classified as relatively flexible polymerases. Pol II can be considered more sterically sensitive (more rigid) than pol IV, with a 33-fold drop in efficiency on increasing template base size from dL to dI as compared with a 7.5-fold drop for the latter. Interestingly, this 7.5-fold drop in efficiency for pol IV is identical to that measured previously for the related archaeal enzyme Dpo4 (25). This is in marked contrast to the rigidity found for two high-fidelity A family polymerases, where a drop of 89-fold in efficiency was found for T7 DNA polymerase (24) and an even larger 160-fold drop for Klenow fragment of DNA pol I (23) in this same sequence context. Both pol II and IV show the same size preference as other polymerases, with a maximum in efficiency at dichlorotoluene, and lower efficiency both for smaller and larger analogs, which suggests that the active site size in the closed conformation is similar, and suggests that the differences in steric responsiveness arise from differential ability to flex inward or outward to adjust to varied substrate size or shape (23–25).

The experiments also clearly show that electrostatic and solvation effects are very important for both pols II and IV, in contrast to the insensitivity to these effects found previously for A family polymerases. Comparison of activities with nonpolar analogs difluorotoluene (or dichlorotoluene) to those with thymine in the template DNA show that pol II loses a large fraction of its activity (by a factor of 1600 in V_{max}/K_m) on making the polar-to-nonpolar

change, while pol IV appears to be even more dependent on the electrostatics of thymine (2900-fold effect for the same change). Similar effects have been observed for Dpo4 and the human Y-family polymerases eta and kappa (25,28,29). The electrostatic charges in the template are also very important for fidelity: the nonpolar template bases are processed with both enzymes with low fidelity (correct base pair preference of 12-fold for pol IV and 37-fold for pol II), whereas thymine yields much higher fidelity for both (4200 and 6100-fold respectively). As a whole, then, we conclude that both enzymes depend on electrostatic interactions to gain the majority of their efficiency and fidelity in synthesis of a new base pair, and that their reliance on steric selectivity is considerably less (intermediate steric selectivity for pol II and low selectivity for pol IV). This is in strong contrast to the A family DNA polymerases pol I and T7 pol, which have shown near wild-type efficiency with nonpolar template bases, and which appear to rely nearly entirely on steric rigidity for their fidelity (23,24,29).

One very great difference between pol II and pol IV is that the latter accepts the nonpolar analogs as dNTP derivatives extremely poorly (as does pol kappa, a possible ortholog (30, 31), while pol II accepts them with even better activity than natural dTTP. Thus for pol II it is clear that the lack of hydrogen bonds in a L-A or F-A base pair does not affect this enzyme's efficiency. We have not observed this large asymmetry (i.e., nonpolar bases being readily accepted as dNTPs but having poor efficiency as template bases) before in other polymerases, although pol II is the first B family enzyme studied kinetically with nonpolar nucleoside isosteres. One possible explanation for the remarkable electrostatic asymmetry in this enzyme is that desolvation of the incoming dNTP in some way relies on polar groups of the template base; this would explain why nonpolar dNTP is a good substrate while the nonpolar template is an extremely poor substrate. Alternatively, it is possible that asymmetry in the active site causes nonpolar bases in the template strand to be misaligned in some way that prevents dNTP insertion. Structural studies of the related B-family RB69 polymerase with DNA and dNTP bound (32–34) indicate that the template base of the terminal pair undergoes minor groove water-mediated interaction with a tyrosine, while the primer terminal base has no polar interaction. It is possible that this electrostatic asymmetry may be related either to misalignment or to asymmetric desolvation. Similar structural asymmetry might be present in pol II; although this enzyme reportedly has been crystallized (35), the structure has not yet been published. Some related polymerases (but lacking DNA and dNTP) have also been studied crystallographically (36–38).

One mechanism by which pol IV achieves adaptive mutations and bypasses damage is through base slippage, leading to -1 frameshift mutations (39). Our current experiments do not show evidence that this mechanism is operating when nonpolar base analogs are in the template. If base slippage were in play for the unnatural template base analogs, we would expect to see dCTP incorporation, as the next template base is G (Figure 5). However, dCTP incorporation was not observed at all, implying that base slippage is not used to bypass these nonpolar bases. This is somewhat unexpected in light of the fact that dATP, the "correct" dNTP, was poorly incorporated.

The current experiments suggest that hydrogen bonding groups in the incipient base pair may be highly important for the damage response activity of DNA pol IV. This polymerase is known to replicate past bulky template adducts such as those with benzo(*a*)pyrene diol epoxide. A crystal structure of this adduct with the related Dpo4 enzyme and an incoming dTTP showed two different conformations (40). In one, the benzo(*a*)pyrene diol was intercalated and the base pairing between dTTP and the terminal A was distorted such that only a single hydrogen bond is formed. In the other conformation, the benzo(*a*)pyrene diol was in the major groove and the face bearing the diol was packed perpendicular to the plane of the base pairs, while the nonpolar face was fully exposed to solvent. In this positioning, hydrogen bonding between the incipient base pair can occur normally. The authors suggested that the nucleotidyl transfer reaction could

only proceed in this latter conformation and not when the adduct intercalates the DNA. Our experiments are in agreement with this hypothesis, and suggest that this enzyme in general should be more proficient at processing adducts that can retain normal hydrogen bonding (and solvation) potential than those that cannot (such as ethenocytosine or ethenoadenine). Moreover, the high steric flexibility of the enzyme would allow for differently-shaped and –sized damaged bases to proceed through the active site successfully. Recent studies of temperature effects on the Dpo4 polymerase also point to flexibility as an important factor in processing a bulky lesion (41).

A similar assessment may be made about the ability of DNA pol II to process damaged DNA templates. Pol II can allow replication bypass for certain DNA lesions including abasic sites, N^4-ethenocytosine, 2-acetylaminofluorene, and some crosslinking lesions (6,42–44). Aside from abasic sites, all of these lesions are polar and may not lead to disruption of electrostatic interactions between water and the template base, which the current studies suggest are important.

Cellular studies using a phage replication assay in *E. coli* showed that the bacterium is able to replicate templates containing the variably-sized nonpolar thymidine analog series (23). It was found that the replication machinery processed non-hydrogen-bonding thymidine analogs with relatively high efficiency, but that the efficiency and fidelity varied strongly with the incremental size changes. Indeed, the most efficient analog (dL) was processed as thymine with relatively high fidelity of 1 error in 1000. The data presented here suggest that pol II and pol IV are most likely not the polymerases responsible for this activity, unless *in vivo* activity is very different from what we have observed *in vitro*. Pol I Klenow fragment was shown to insert dATP opposite dF and dL with high efficiency and fidelity (11,23), which suggests that pol I is a better candidate than the above enzymes for the observed activity. It remains to be seen how the other *E. coli* polymerases (III and V) would respond to systematic changes in electrostatics and sterics in their active sites.

Experimental Section

Nonpolar thymidine analogs were synthesized as reported previously (21,22). Pol II (exo-) and pol IV were purified as described (3,27). For steady-state single nucleotide incorporation experiments, a 28-mer/23-mer template/primer duplex with the sequence (5′-TAATACGACTCACTATAGGGAGA) · (5′-ACTGXTCTCCCTATAGTGAGTCGTATTA) was used as a polymerase substrate for insertion kinetics. A 24-mer primer with the sequence (5′-TAATACGACTCACTATAGGGAGAA) was used for extension kinetics. Primers were ^{32}P end-labeled at the 5′ terminus with [γ-^{32}P]ATP (Amersham Bioscience) and T4 polynucleotide kinase (Invitrogen). Labeled primers were purified using spin columns (Biorad). Primer-templates were annealed by making a 1:1 mixture of primer and template (4 mM each) in buffer containing 20 mM Tris (pH 7.5), 20 mM sodium glutamate, 4% v/v glycerol, 8 mM $MgCl_2$, and 5 mM DTT, then heating to 95 °C and slowly cooling to 4 °C over 90 min. The primer-template solution was then mixed with 4x enzyme solution to make a 2× primer-template-enzyme solution.

Primer-template-enzyme solution was mixed with 2x dNTP solution and the reactions were incubated at 37 °C. Reactions were quenched by addition of stop buffer (95% formamide containing 10 mM EDTA, 0.05% xylene cyanol and 0.05% bromophenol blue). Typical reaction conditions used 1.5 – 29 μg/mL of pol II or 2 – 40 μg/mL of pol IV and 0.5 – 30 min reaction time.

Products were resolved from unreacted primer by 20% denaturing polyacrylamide gel electrophoresis and quantified by autoradiography using a phosphorimager (Molecular

Dynamics). Spot intensities on the imaged gels were calculated using ImageQuant (Molecular Dynamics). Reaction velocity *v* for individual reactions was calculated by the equation $v = I_{n+1}/(I_n+I_{n+1})/t$, where I_n is the intensity of the unreacted primer band and I_{n+1} is the intensity of the product band. Velocities were normalized for enzyme concentration, and V_{max} and K_M values were determined from Hanes-Woolf plots.

Supplementary Material

Refer to Web version on PubMed Central for supplementary material.

Acknowledgements

This work was support by the U.S. National Institutes of Health (GM072705 to ETK and R37GM21422 and ES012259 to MFG). APS acknowledges support from an NSF Graduate Fellowship and a Lieberman Fellowship.

References

1. Latham GJ, McNees AG, De Corte B, Harris CM, Harris TM, O'Donnell M, Lloyd RS. Comparison of the efficiency of synthesis past single bulky DNA adducts in vivo and in vitro by the polymerase III holoenzyme. Chem Res Toxicol 1996;9:1167–1175. [PubMed: 8902273]
2. Rangarajan S, Woodgate R, Goodman MF. Replication restart in UV-irradiated Escherichia coli involving pols II, III, V, PriA, RecA and RecFOR proteins. Mol Microbiol 2002;43:618–628.
3. Kobayashi S, Valentine MR, Pham P, O'Donnell M, Goodman MF. Fidelity of Escherichia coli DNA polymerase IV. J Biol Chem 2002;277:34198–34207. [PubMed: 12097328]
4. Wang Z, Lazarov E, O'Donnell M, Goodman MF. Resolving a fidelity paradox. J Biol Chem 2002;277:4446–4454. [PubMed: 11733526]
5. Goodman MF. Error-prone repair DNA polymerases in prokaryotes and eukaryotes. Annu Rev Biochem 2002;71:17–50. [PubMed: 12045089]
6. Napolitano R, Janel-Bintz R, Wagner J, Fuchs RPP. All three SOS-inducible DNA polymerases (Pol II, Pol IV and Pol V) are involved in induced mutagenesis. EMBO J 2000;19:6259–6265. [PubMed: 11080171]
7. Kim SR, Matsui K, Yamada M, Gruz P, Nohmi T. Roles of chromosomal and episomal dinB genes encoding DNA pol IV in targeted and untargeted mutagenesis in Escherichia coli. Mol Genet Genomics 2001;266:207–215. [PubMed: 11683261]
8. Delmas S, Matic I. Interplay between replication and recomination in Escherichia coli: impact of the alternative DNA polymerases. Proc Natl Acad Sci U S A 2006;103:4564–4569. [PubMed: 16537389]
9. McKenzie GJ, Lee PL, Lombardo MJ, Hastings PJ, Rosenberg SM. SOS mutator DNA polymerase IV functions in adaptive mutation and not adaptive amplification. Mol Cell 2001;7:571–579. [PubMed: 11463382]
10. Kool ET. Active site tightness and substrate fit in DNA replication. Annu Rev Biochem 2002;69:497–529.
11. Moran S, Ren RXF, Rummey S IV, Kool ET. Difluorotoluene, a nonpolar isostere for thymidine, codes specifically and efficiently for adenine in DNA replication. J Am Chem Soc 1997;119:2056–2057.
12. Kool ET, Sintim HO. The difluorotoluene debate - a decade later. Chem Commun 2006;35:3665–3675.
13. Matray TJ, Kool ET. A specific partner for abasic damage in DNA. Nature 1999;399:704–708. [PubMed: 10385125]
14. Kool ET. Replication of non-hydrogen bonded bases by DNA polymerases: a mechanism for steric matching. Biopolymers (Nucl Acid Sci) 1998;48:3–17.
15. Echols H, Goodman MF. Fidelity mechanisms in DNA-replication. Annu Rev Biochem 1991;60:477–511. [PubMed: 1883202]
16. Schweitzer BA, Kool ET. Aromatic nonpolar nucleosides as hydrophobic isosteres of pyrimidines and purine nucleosides. J Org Chem 1994;59:7238–7242.

17. Morales JC, Kool ET. Efficient replication between non-hydrogen-bonded nucleoside shape analogs. Nat Struct Biol 1998;5:950–954. [PubMed: 9808038]
18. Ogawa AK, Wu YQ, Berger M, Schultz PG, Romesberg FE. Rational design of an unnatural base pair with increased kinetic selectivity. J Am Chem Soc 2000;122:8803–8804.
19. Sintim HO, Kool ET. Remarkable sensitivity to DNA base shape in the DNA polymerase active site. Angew Chem Intl Ed 2006;45:1974–1979.
20. Hirao I, Kimoto M, Mitsui T, Fujiwara T, Kawai R, Sato A, Harada Y, Yokoyama S. An unnatural hydrophobic base pair system: site-specific incorporation of nucleotide analogs into DNA and RNA. Nat Methods 2006;3:729–735. [PubMed: 16929319]
21. Kim TW, Kool ET. A set of nonpolar thymidine nucleoside analogues with gradually increasing size. Org Lett 2004;6:3949–3952. [PubMed: 15496071]
22. Kim TW, Kool ET. A series of nonpolar thymidine analogs of increasing size: DNA base pairing and stacking properties. J Org Chem 2005;70:2048–2053. [PubMed: 15760186]
23. Kim TW, Delaney JC, Essigmann JM, Kool ET. Probing the active site tightness of DNA polymerase in subangstrom increments. Proc Natl Acad Sci U S A 2005;102:15803–15808. [PubMed: 16249340]
24. Kim TW, Brieba LG, Ellenberger T, Kool ET. Functional evidence for a small and rigid active site in a high fidelity DNA polymerase. J Biol Chem 2006;281:2289–2295. [PubMed: 16311403]
25. Mizukami S, Kim TW, Helquist SA, Kool ET. Varying DNA base-pair size in subangstrom increments: evidence for a loose, not large, active site in low-fidelity Dpo4 polymerase. Biochemistry 2006;45:2772–2778. [PubMed: 16503632]
26. Kobayashi S, Valentine MR, Pham P, O'Donnell M, Goodman MF. Fidelity of Escherichia coli DNA polymerase IV. J Biol Chem 2002;277:34198–207. [PubMed: 12097328]
27. Cai H, Yu H, McEntee K, Kunkel TA, Goodman MF. Purification and properties of wild-type and exonuclease-deficient DNA polymerase II from Escherichia coli. J Biol Chem 1995;270:15327–15335. [PubMed: 7797520]
28. Washington MT, Helquist SA, Kool ET, Prakash L, Prakash S. Requirement of Watson-Crick hydrogen bonding for DNA synthesis by yeast DNA polymerase eta. Mol Cell Biol 2003;23:5107–5112. [PubMed: 12832493]
29. Summerer D, Marx A. DNA polymerase selectivity: sugar interactions monitored with high-fidelity nucleotides. Angew Chem Intl Ed 2001;40:3693–3695.
30. Wolfle WT, Washington MT, Kool ET, Spratt TE, Helquist SA, Prakash L, Prakash S. Evidence for a Watson-Crock hydrogen bonding requirement in DNA synthesis by human DNA polymerase kappa. Mol Cell Biol 2005;25:7137–7143. [PubMed: 16055723]
31. Lee CH, Chandani S, Loechler EL. Humology modeling of four Y-family, lesion-bypass DNA polymerases: The case that E. coli Pol IV and human Pol kappa are orthologs, and E. coli Pol V and human Pol eta are orthologs. J Mol Graph Model 2006;25:87–102. [PubMed: 16386932]
32. Franklin MC, Wang J, Steitz TA. Structure of the replicating complex of a Pol α family DNA polymerase. Cell 2001;105:657–667. [PubMed: 11389835]
33. Hogg M, Wallace SS, Doublie S. Crystallographic snapshots of a replicative DNA polymerase encountering an abasic site. EMBO J 2004;23:1483–1493. [PubMed: 15057283]
34. Freisinger E, Grollman AP, Miller H, Kisker C. Lesion (in)tolerance reveals insights into DNA replication fidelity. EMBO J 2004;23:1494–1505. [PubMed: 15057282]
35. Anderson WF, Prince DB, Yu H, McEntee K, Goodman MF. Crystallization of DNA polymerase II from Escherichia coli. J Mol Biol 1994;238:120–122. [PubMed: 8145251]
36. Hashimoto H, Nishioka M, Fujiwara S, Takagi M, Imanaka T, Inoue T, Kai Y. Crystal structure of DNA polymerase from hyperthermophilic archaeon Pyrococcus kodakaraensis KOD1. J Mol Biol 2001;306:469–477. [PubMed: 11178906]
37. Wang J, Sattar AK, Wang CC, Karam JD, Konigsberg WH, Steitz TA. Crystal structure of a pol alpha family replication DNA polymerase from bacteriophage RB69. Cell 1997;89:1087–1099. [PubMed: 9215631]
38. Zhao Y, Jeruzalmi D, Moarefi I, Leighton L, Lasken R, Kuriyan J. Crystal structure of an archaebacterial DNA polymerase. Structure 1999;7:1189–1199. [PubMed: 10545321]

39. Kim SR, Maenhaur-Michel G, Yamada M, Yamamoto Y, Matsui K, Sofuni T, Nohmi T, Ohmori H. Multiple pathways for SOS-induced matagenesis in Escherichia coli: an overexpression of dinB/dinP results in strongly enhancing mutagenesis in the absence of any exogenous treatment to damage DNA. Proc Natl Acad Sci U S A 1997;94:13792–13797. [PubMed: 9391106]

40. Ling H, Sayer JM, Plosky BS, Yagi H, Boudsocq F, Woodgate R, Jerina DM, Yang W. Crystal structure of a benzo[a]pyrene diol epoxide adduct in a ternary complex with a DNA polymerase. Proc Natl Acad Sci U S A 2004;101:2265–2269. [PubMed: 14982998]

41. Perlow-Poehnelt RA, Likhterov I, Wang LH, Scicchitano DA, Geacintov NE, Broyde S. Increased flexibility enhances misincorporation - Temperature effects on nucleotide incorporation opposite a bulky carcinogen-DNA adduct by a Y-family DNA polymerase. J Biol Chem 2007;282:1397–1408. [PubMed: 17090533]

42. Paz-Elizur T, Takeshita M, Goodman MF, O'Donnell M, Livneh Z. Mechanism of translesion DNA synthesis by DNA polymerase II. Comparison to DNA polymerases I and III core. J Biol Chem 1996;271:24662–24669. [PubMed: 8798733]

43. Fuchs RP, Koffel-Schwartz N, Pelet S, Janel-Bintz R, Napolitano R, Becherel OJ, Broschard TH, Burnouf DY, Wagner J. DNA polymerases II and V mediate respectively mutagenic (-2 frameshift) and error-free bypass of a single N-2-acetylaminofluorene adduct. Biochem Soc Trans 2001;29:191–195. [PubMed: 11356152]

44. Kanuri M, Nechev LV, Kiehna SE, Tamura PJ, Harris CM, Harris TM, Lloyd RS. Evidence for Escherichia coli polymerase II mutagenic bypass of intrastrand DNA crosslinks. DNA Repair (Amst) 2005;4:1374–1380. [PubMed: 16257273]

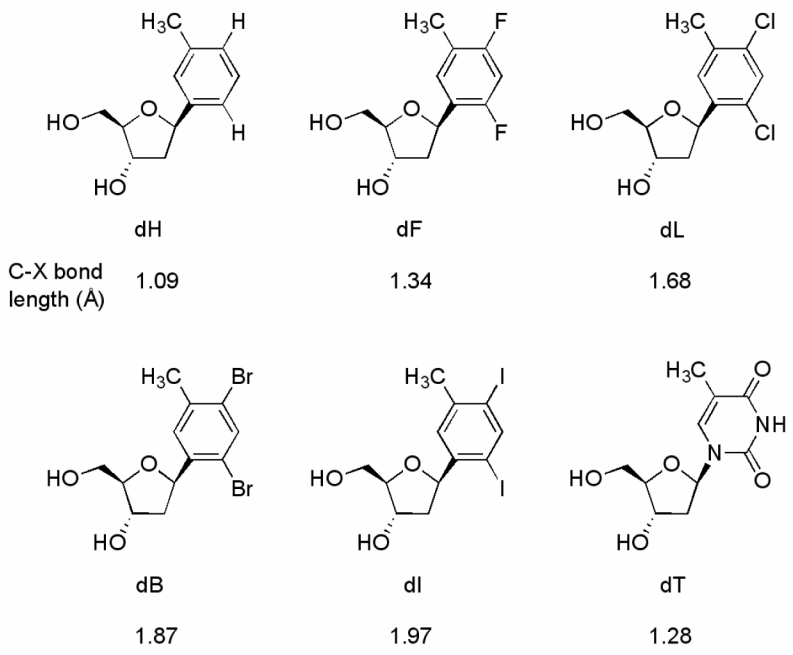

Figure 1.
Structures of nonpolar thymidine analogs of varied size used in this study.

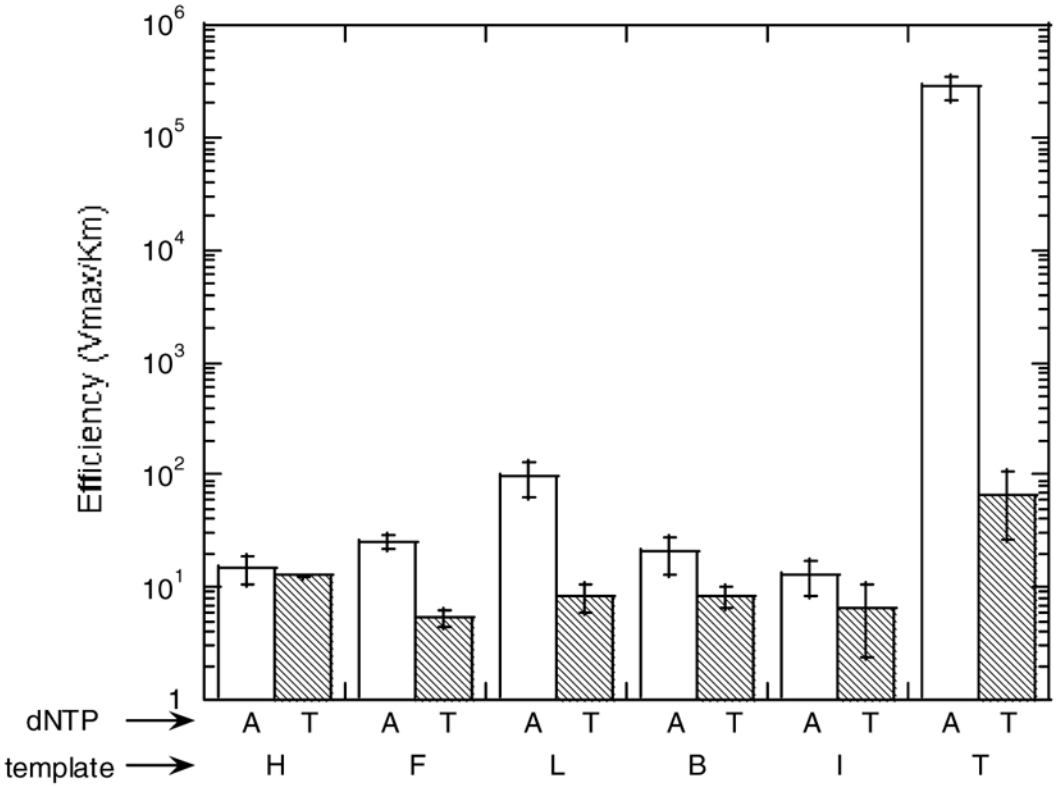

Figure 2.

Steady-state efficiencies (V_{max}/K_M) for insertion of natural dNTPs opposite template base analogs of increasing size for DNA pol IV. Note log scale of efficiencies. Primer-template duplexes had the sequence (5′-TAATACGACTCACTATAGGGAGA) · (5′-ACTGXTCTCCCTATAGTGAGTCGTATTA). Kinetics were measured at 37 °C in a buffer containing 20 mM Tris (pH 7.5), 20 mM sodium glutamate, 4% v/v glycerol, 8 mM $MgCl_2$, and 5 mM DTT. The primer was 5′-end labeled with γ-^{32}P-ATP and was extended by the polymerase in the presence of a single dNTP over various concentrations and times; products of single nucleotide insertions were resolved from unreacted primer by 20% denaturing polyacrylamide gel electrophoresis and quantified by autoradiography. See Table 1 for numerical data.

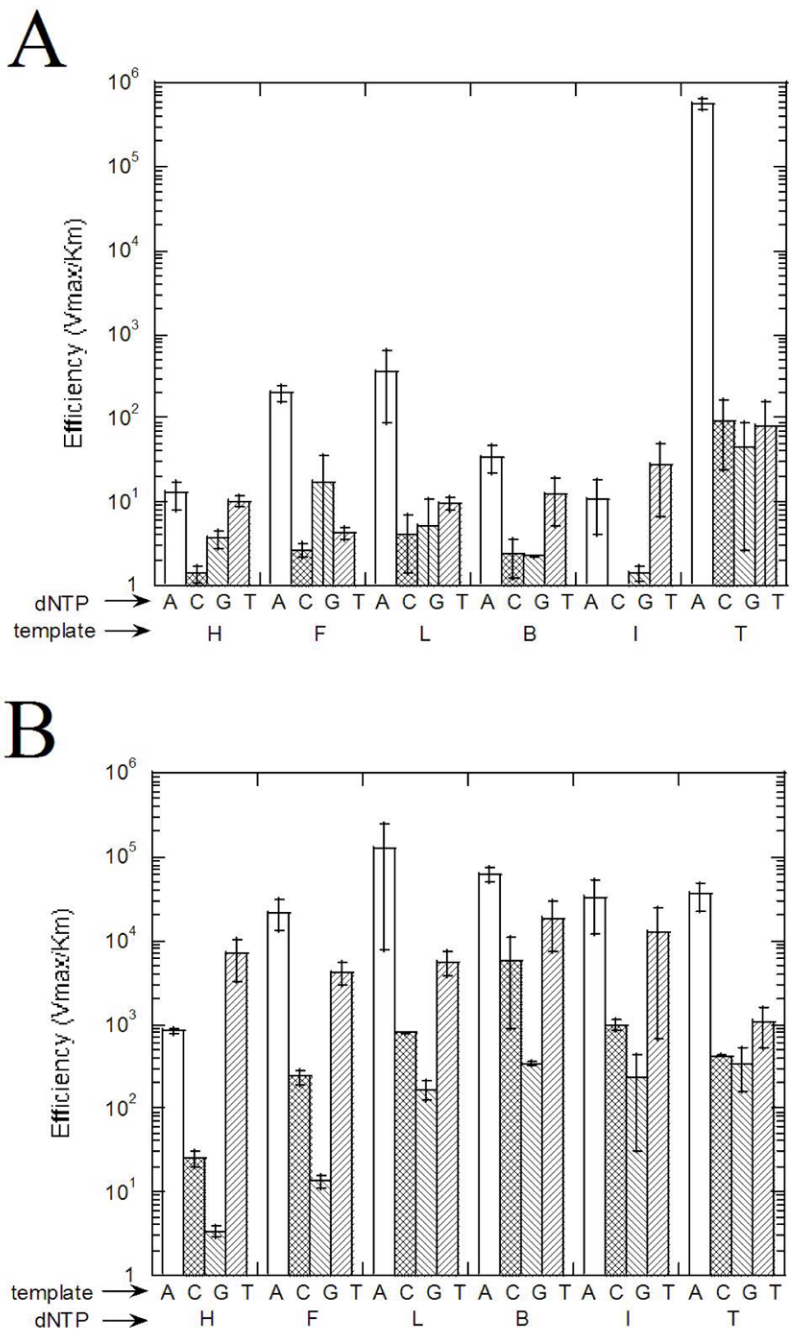

Figure 3.

The effects of varying base size on DNA pol II. Single nucleotide insertion efficiencies (V_{max}/K_M) are shown on a log scale. (A) Insertion of natural dNTPs opposite template base analogs of increasing size, with T for comparison. (B) Insertion of nucleoside triphosphate analogs of increasing size opposite natural template bases, with dTTP for comparison. Conditions are the same as for Figure 2. See Tables 2 and 3 for data.

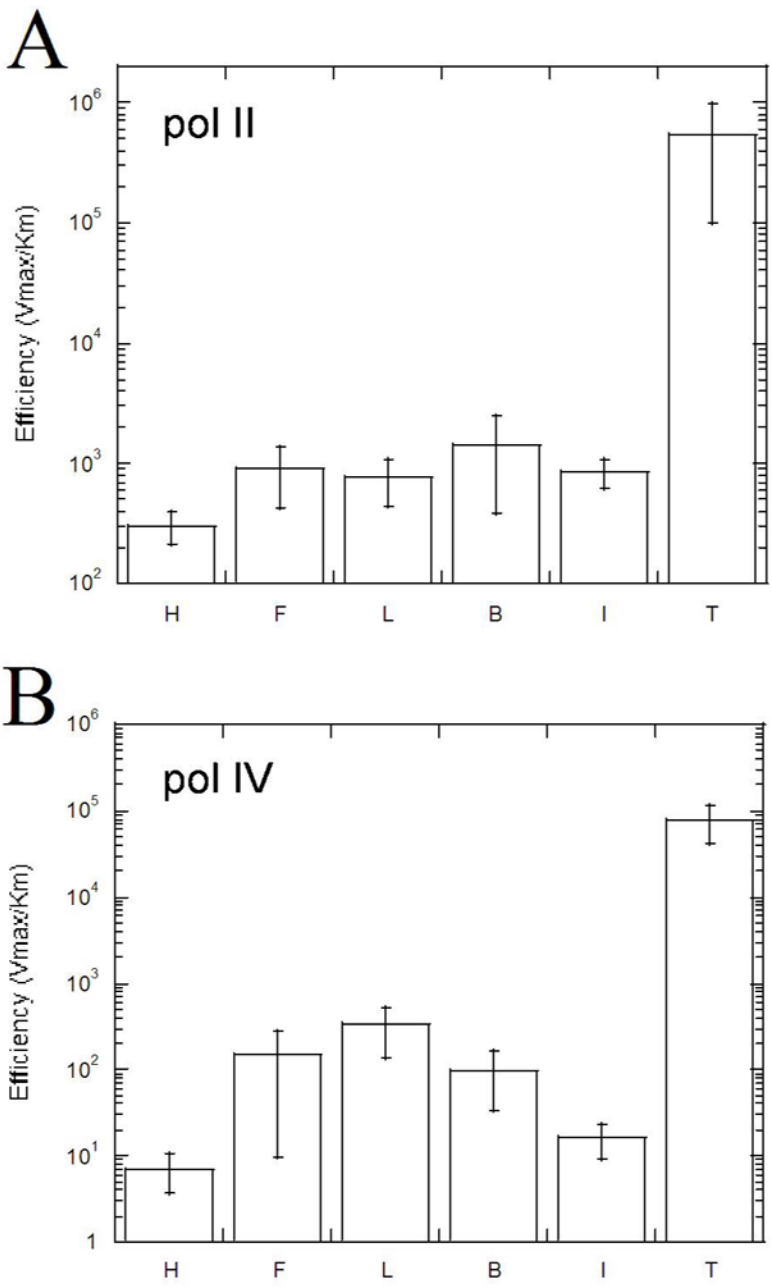

Figure 4.

Efficiencies (V_{max}/K_M) versus base size for extension past an A·X base pair, where X is a nonpolar thymidine of variable size in the template strand. (A) Extension by DNA pol II. (B) Extension by pol IV. Primer-template duplexes had the sequence (5′-TAATACGACTCACTATAGGGAGAA) · (5′-ACTGXTCTCCCTATAGTGAGTCGTATTA). Other conditions are described in the Figure 2 legend. See Tables 4 and 5 for data.

Figure 5.
Sketch showing a potential frameshift caused by DNA slippage. (A) Normal nucleotide incorporation geometry. (B) Possible incorporation geometry with unnatural base slipped out, leading to a -1 frameshift mutation. No evidence for the frameshift mode was seen with nonnatural template bases.

Table 1

Steady-state kinetics data for DNA pol IV insertion of natural dNTPs opposite variably-sized nonnatural template thymine analogs.[a,b]

dNTP	Template Base	V_{max} (%·min^{-1})	K_M (μM)	Efficiency (V_{max}/K_M)	f_{inc}
dATP	H	0.0075 (0.0023)	580 (370)	1.5×10^{1} (0.4)	5.4×10^{-5}
	F	0.0051 (0.0008)	210 (20)	2.5×10^{1} (0.3)	8.9×10^{-5}
	L	0.017 (0.005)	190 (70)	9.7×10^{1} (3.3)	3.5×10^{-4}
	B	(0.013 (0.004)	750 (550)	2.0×10^{1} (0.8)	7.1×10^{-5}
	I	0.0072 (0.0060)	790 (950)	1.3×10^{1} (0.5)	4.6×10^{-5}
	T	2.2 (0.2)	8.2 (2.2)	2.8×10^{5} (0.7)	1
dTTP	H	0.0051 (0.0004)	400 (20)	1.2×10^{1} (0.1)	4.3×10^{-5}
	F	0.0057 (0.0002)	1100 (200)	5.4 (0.9)	1.9×10^{-5}
	L	0.0064 (0.0012)	810 (280)	8.4 (2.4)	3.0×10^{-5}
	B	0.0028 (0.0004)	330 (30)	8.4 (1.9)	3.0×10^{-5}
	I	0.0041 (0.0032)	970 (1100)	6.5 (4.1)	2.3×10^{-5}
	T	0.012 (0.005)	250 (220)	6.7×10^{1} (4.1)	2.3×10^{-4}

[a] Values in parentheses indicate standard deviations from multiple experiments.

[b] f_{inc} is calculated as the ratio of apparent V_{max}/K_m relative to the A->T case.

Table 2

Steady-state kinetics data for DNA pol II insertion of natural dNTPs opposite variably-sized nonnatural template thymine analogs.[a]

dNTP	Template Base	V_{max} (%·min^{-1})	K_M (μM)	Efficiency (V_{max}/K_M)	f_{inc}
dATP	H	0.0019 (0.0007)	150 (10)	1.2×10^1 (0.5)	2.1×10^{-5}
	F	0.018 (0.010)	86 (32)	2.0×10^2 (0.5)	3.5×10^{-4}
	L	0.027 (0.019)	74 (3)	3.6×10^2 (2.7)	6.3×10^{-4}
	B	0.0054 (0.0011)	160 (20)	3.4×10^1 (1.2)	6.0×10^{-5}
	I	0.0046 (0.0030)	430 (10)	1.1×10^1 (0.7)	1.9×10^{-5}
	T	0.12 (0.06)	0.19 (0.09)	5.7×10^5 (0.8)	1
dCTP	H	0.00078 (0.00004)	580 (160)	1.4 (0.3)	2.5×10^{-6}
	F	0.00045 (0.00025)	170 (60)	2.6 (0.5)	4.6×10^{-6}
	L	0.00042 (0.00024)	100 (10)	4.1 (2.7)	7.2×10^{-6}
	B	0.00040 (0.00009)	180 (50)	2.4 (1.1)	4.2×10^{-6}
	I	*b*	*b*	*b*	-
	T	0.0077 (0.0046)	87 (16)	9.4×10^1 (7.0)	1.6×10^{-4}
dGTP	H	0.0023 (0.0006)	630 (10)	3.7 (0.8)	6.5×10^{-6}
	F	0.0044 (0.0059)	170 (160)	1.7×10^1 (1.8)	3.0×10^{-5}
	L	0.0025 (0.0012)	690 (450)	5.2 (5.1)	9.1×10^{-6}
	B	0.00069 (0.00065)	310 (290)	2.2 (0.1)	3.9×10^{-6}
	I	0.00037 (0.00030)	300 (280)	1.4 (0.3)	2.5×10^{-6}
	T	0.012 (0.005)	370 (230)	4.5×10^1 (4.2)	7.9×10^{-5}
dTTP	H	0.0066 (0.0042)	690 (520)	1.0×10^1 (0.1	1.8×10^{-5}
	F	0.0018 (0.0008)	420 (120)	4.2 (0.8)	7.4×10^{-6}
	L	0.0019 (0.0009)	190 (60)	9.7 (1.6)	1.7×10^{-5}
	B	0.0046 (0.0015)	500 (410)	1.2×10^1 (0.7)	2.1×10^{-5}
	I	0.0076 (0.0010)	370 (240)	2.8×10^1 (2.1)	4.9×10^{-5}
	T	0.0045 (0.0036)	72 (28)	7.9×10^1 (8.1)	1.4×10^{-4}

[a] Values in parentheses indicate standard deviations from multiple experiments.

[b] No incorporation observed with 29 μg/mL enzyme and 30 min reaction time.

Table 3

Steady-state kinetics data for DNA pol II insertion of nonnatural dNTPs opposite natural template bases.[a]

Template Base	dNTP	V_{max} (%·min^{-1})	K_M (μM)	Efficiency (V_{max}/K_M)	f_{inc}
A	dHTP	0.12 (0.009)	140 (20)	8.3×10^{2} (0.7)	2.3×10^{-2}
	dFTP	0.43 (0.10)	21 (0.4)	2.2×10^{4} (0.9)	6.1×10^{-1}
	dLTP	0.45 (0.06)	5.8 (5.0)	1.3×10^{5} (1.2)	3.6
	dBTP	0.39 (0.16)	6.7 (3.9)	6.1×10^{4} (1.2)	1.7
	dITP	0.21 (0.01)	8.3 (5.1)	3.2×10^{4} (2.1)	8.9×10^{-1}
	dTTP	0.39 (0.20)	11 (2)	3.6×10^{4} (1.3)	1
C	dHTP	0.0034 (0.0005)	140 (10)	2.5×10^{1} (0.6)	6.9×10^{-4}
	dFTP	0.024 (0.001)	100 (10)	2.4×10^{2} (0.4)	6.7×10^{-3}
	dLTP	0.028 (0.0014)	36 (3)	7.9×10^{2} (0.3)	2.2×10^{-2}
	dBTP	0.017 (0.0003)	4.6 (3.9)	5.8×10^{3} (5.0)	1.6×10^{-1}
	dITP	0.0055 (0.0014)	5.5 (0.7)	1.0×10^{3} (0.1)	2.8×10^{-2}
	dTTP	0.055 (0.0005)	130 (10)	4.2×10^{2} (0.2)	1.2×10^{-2}
G	dHTP	0.00021 (0.00008)	66 (33)	3.3 (0.5)	9.2×10^{-5}
	dFTP	0.00066 (0.00012)	50 (1)	1.3×10^{1} (0.2)	3.6×10^{-4}
	dLTP	0.0031 (0.0007)	20 (9)	1.7×10^{2} (0.4)	4.7×10^{-3}
	dBTP	0.0057 (0.0028)	17 (9)	3.4×10^{2} (0.2)	9.4×10^{-3}
	dITP	0.0024 (0.0001)	17 (15)	2.3×10^{2} (2.0)	6.4×10^{-3}
	dTTP	0.048 (0.020)	140 (80)	3.3×10^{2} (1.8)	9.2×10^{-3}
T	dHTP	0.0093 (0.0078)	1.9 (2.1)	6.9×10^{3} (3.6)	1.9×10^{-1}
	dFTP	0.014 (0.004)	3.5 (2.0)	4.2×10^{3} (1.2)	1.2×10^{-1}
	dLTP	0.041 (0.017)	7.2 (0.6)	5.5×10^{3} (1.9)	1.5×10^{-1}
	dBTP	0.084 (0.036)	6.3 (5.7)	1.8×10^{4} (1.1)	5.0×10^{-1}
	dITP	0.051 (0.018)	6.2 (4.4)	1.3×10^{4} (1.2)	3.6×10^{-1}
	dTTP	0.013 (0.005)	12 (2)	1.1×10^{3} (0.5)	3.1×10^{-2}

[a] Values in parentheses indicate standard deviations from multiple experiments.

Table 4

Steady-state kinetics data for extension beyond variably-sized base pairs by DNA pol II.[a,b]

Terminal Base Pair	V_{max}(%·min^{-1})	K_M (μM)	Efficiency (V_{max}/K_M)	f_{ext}
A·H	0.013 (0.008)	49 (43)	3.0×10^2 (0.9)	5.6×10^{-4}
A·F	0.013 (0.008)	14 (2)	9.1×10^2 (4.8)	1.7×10^{-3}
A·L	0.022 (0.007)	34 (24)	7.5×10^2 (3.2)	1.4×10^{-3}
A·B	0.029 (0.018)	34 (37)	1.4×10^3(1.0)	2.6×10^{-3}
A·I	0.025 (0.024)	34 (37)	8.6×10^2 (2.4)	1.6×10^{-3}
A·T	0.13 (0.09)	0.25 (0.04)	5.4×10^5 (4.4)	1

[a] Values in parentheses indicate standard deviations from multiple experiments.

[b] f_{ext} is calculated as the ratio of apparent V_{max}/K_m relative to the A->T case.

Table 5

Steady-state kinetics data for extension beyond variably-sized base pairs by DNA pol IV.[a]

Terminal Base Pair	V_{max} (%·min^{-1})	K_M (μM)	Efficiency (V_{max}/K_M)	f_{ext}
A·H	0.0051 (0.0032)	830 (610)	7.0 (3.3)	9.0×10^{-5}
A·F	0.024 (0.016)	190 (70)	1.5×10^{2} (1.4)	1.9×10^{-3}
A·L	0.071 (0.011)	270 (190)	3.3×10^{2} (2.0)	4.2×10^{-3}
A·B	0.022 (0.002)	280 (160)	9.9×10^{1} (6.6)	1.3×10^{-3}
A·I	0.012 (0.005)	930 (660)	1.6×10^{1} (0.7)	2.1×10^{-4}
A·T	1.3 (0.7)	20 (17)	7.8×10^{4} (3.6)	1

[a] Values in parentheses indicate standard deviations from multiple experiments.